DOI:10.1021/jf904561e

JOURNAL OF AGRICULTURAL AND FOOD CHEMISTRY
ARTICLE

Identification of the Position of Mono-*O*-glucuronide of Flavones and Flavonols by Analyzing Shift in Online UV Spectrum (λ_{max}) Generated from an Online Diode Array Detector

Rashim Singh,[†] Baojian Wu,[†] Lan Tang,[§] Zhongqiu Liu,[§] and Ming Hu*,[†]

[†]Department of Pharmacological and Pharmaceutical Sciences, College of Pharmacy, University of Houston, 1441 Moursund Street, Houston, Texas 77030, and [§]Department of Pharmaceutics, School of Pharmaceutical Sciences, Southern Medical University, Guangzhou, Guangdong, China

The beneficial pharmacological effects of flavonoids such as chemoprevention against cancer, aging, and heart diseases are severely limited due to their extensive in vivo glucuronidation by UDP-glucuronosyltransferases (UGTs). UGTs showed regiospecificity (i.e., position preference) in the glucuronidation of the flavonoids based on the substrate's chemical structure. In this paper, glucuronide(s) of 36 flavones and flavonols were generated using an in vitro glucuronidation reaction. UPLC/MS/MS was used to confirm the degree (mono- or di-) of glucuronidation in flavonoids with up to four hydroxyl groups. UV spectra of flavonoids and their respective mono-*O*-glucuronides were generated using UPLC with an online diode array detector. Analysis of the extent of shift in spectra of glucuronides in band I (300−385 nm) and band II (240−280 nm) regions as reflected by changes in λ_{max} value was used to identify the position of glucuronidation. The data showed that glucuronidation of the 3- and 4′-hydroxyls resulted in band I λ_{max} hypsochromic shifts (or blue shift) of 13−30 and 5−10 nm, respectively. Glucuronidation of the 5-hydroxyl group caused a band II λ_{max} hypsochromic shift of 5−10 nm. In contrast, glucuronidation of the 7-hydroxyl group did not cause any λ_{max} change in band I or II λ_{max}, whereas glucuronidation of the 6-hydroxyl group did not cause predictable changes in λ_{max} values. The paper demonstrated for the first time that a rapid and robust analysis method using λ_{max} changes in online UV spectra can be used to pinpoint region-specific glucuronidation of flavones and flavonols with hydroxyl groups at the 4′-, 3-, 5-, and/or 7-position(s).

KEYWORDS: Flavonoids; glucuronide position; UPLC; UGT regiospecific

INTRODUCTION

Flavonoids are a class of phytochemicals widely distributed in the plant world and are believed to possess a myriad of beneficial effects, but their poor bioavailabilities have severely limited their potentials as agents that can be developed as drugs (*1*−*8*). This is because low bioavailabilities mean large variability in individual exposure, which would require a larger population for clinical trials to demonstrate effectiveness (*7*−*13*). The extensive metabolism of flavonoids by glucuronidation is the main reason for their poor in vivo bioavailabilities, with sulfation designated the secondary contributing factor (*10*, *11*, *14*). O-methylation has also been reported as a contributing metabolic pathway for various flavonoids (*15*). Phase II metabolism is considered as the major detoxification pathway in the human body. Usually, the addition of glucuronic acid and a sulfate moiety to the structure of flavonoids through glucuronidation and sulfation reactions makes the flavonoids more hydrophilic, which can then be eliminated through bile and the kidney (*16*, *17*).

To overcome the problem of their low bioavailabilities, it is becoming increasingly urgent to understand the structure−metabolism relationship (SMR) between flavonoids and various UDP-glucuronosyltransferase (or UGT) isoforms. However, development of this understanding had been impeded by the lack of UGT crystal structure and very limited qualitative and quantitative information about the regiospecific glucuronidation of large numbers of structurally diverse flavonoids.

Approximately 150 papers on the topic of flavonoid glucuronidation have been published since 2000, which is 20% of the total number of glucuronidation papers published during that period, according to a PubMed search of UGT and metabolism on October 16, 2009. However, it was interesting to note that only 10−15% of the published literature on flavonoid glucuronidation had information about the position of flavonoid glucuronides, more than half of which were about glucuronides of a single flavonol, quercetin. We hypothesized that this was because most laboratories did not have access to a convenient method that could identify the position of glucuronidation.

*Address correspondence to this author at Department of Pharmaceutical Sciences, College of Pharmacy, University of Houston, 1441 Moursund St., Houston, TX 77030 [phone (713) 795-8320; e-mail mhu@uh.edu].

 Published on Web 08/05/2010

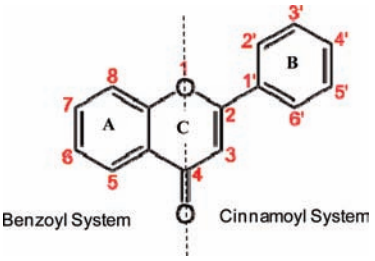

Figure 1. Backbone of selected flavonoids used for the present study with one or more hydroxyl and/or methoxyl group substitutions. In this paper, the term "flavonoid" has been used to represent the compounds from subclasses flavone and flavonol only. Band I was considered to be associated with absorption due to the B-ring cinnamoyl system (mark), and band II with absorption due to the A-ring benzoyl system (mark).

NMR would be one of the best, if not the best, methods to determine the position of glucuronidation in a flavonoid. In an earlier paper from this laboratory, we identified the position of prunetin glucuronidation via the use of NMR, which is quite time-consuming (*18*). It was affordable to us because only one glucuronide was formed when using a particular UGT (e.g., UGT 1A10) isoform. It would be exceedingly time-consuming and difficult if we had to separate two or more glucuronides using liquid chromatography.

To improve upon this time-consuming method, Brodbelt and co-workers had used positive and negative electrospray ionization mass spectrometry (EI-MS) coupled with collision-induced dissociation (CID) to identify the position of flavonoid glucuronidation (*19*, *20*). This group used EI-MS followed by postcolumn complexation of flavonoid with transition metals such as magnesium(II), cobalt(II), and nickel(II) and auxiliary ligands such as 4,7-dimethyl-1,10-phenanthroline and 4,7-diphenyl-1,10-phenanthroline. Upon CID, this complex yielded product ions that were used to identify the position of glucuronidation (*19*, *20*). Whereas this method significantly advanced our ability to identify the position of glucuronidation, it remains complex and requires the use of complex instrumentation and reagents. On the other hand, this work demonstrated that it is possible to modernize a classical method that used a flavonoid−metal complex to identify the position of glycosylation or glucuronidation using purified flavonoids (*19*−*21*). Other groups have also reported the use of ESI-MS coupled with HPLC-UV for detection of the position of glycosylation or glucuronidation in flavonoids (*21*−*25*).

Recently, we became aware of 1970s literature that showed the position of glycosylation of flavonoids can significantly change the UV spectra of their respective aglycones (*26*). Although the observations were mainly based on work with purified flavonoids with glycosylation (with a variety of sugar moieties at different positions) (*26*), the potential exists to adapt it to modern analytical techniques such as UPLC with online UV spectra without having to first purify the compounds. Because flavones and flavonols are two of the major subclasses of flavonoids, each numbered in the hundreds and commercially available, they were selected as the model compounds for the present study (**Figure 1**), and we used the term "flavonoids" in this paper to represent these two subclasses of flavonoids. They were also selected because they consistently showed (with rare exceptions) two major absorption peaks (or λ_{max}) in the regions of 240−280 nm (commonly referred to as band II) and 300−380 nm (commonly referred to as band I). Spectra of flavones and flavonols (with 3-hydroxyl group) could be differentiated by band I λ_{max}. Band I λ_{max} of flavones occurred at 304−350 nm, whereas that of flavonols occurred at longer wavelengths of 352−385 nm (*26*). Finally, these flavonoids were selected because multiple hydroxyl positions (e.g., 3-, 5-, 7-, and/or 4′-position) may be glucuronidated, which allowed us to determine the preferred position for glucuronidation in a flavonoid with multiple hydroxyl groups. The latter is important because most of the flavonoids in nature have multiple hydroxyl groups.

Therefore, the purpose of this paper is to establish a fast, economical, and easily accessible method to determine the position of mono-O-glucuronidation of flavonols and flavones. We hypothesized that this new method would cost much less with respect to time and efforts and demand less chemistry and mass spectrometry expertise. Such a method should be very helpful in furthering the research of SMR of UGTs and the role of UGT metabolism in drug disposition. It would also raise the quality of future research endeavors in the field of flavonoid metabolism as it would be much easier for other researchers to use the same approach to identify the position of flavonoid glucuronidation.

EXPERIMENTAL PROCEDURES

Expressed human UGT isoforms (Supersomes) 1A1, 1A7, 1A8, 1A9, and 1A10 were purchased from BD Biosciences (Woburn, MA). β-D-Glucuronidase without sulfatase (product G7396), uridine diphosphoglucuronic acid (UDPGA), alamethicin, D-saccharic-1,4-lactone monohydrate, and magnesium chloride were purchased from Sigma-Aldrich (St. Louis, MO). Ammonium acetate (HPLC grade) was purchased from J. T. Baker (Phillipsburg, NT). The UGT isoforms for generating the glucuronides were selected on the basis of preliminary and published studies (*27*) from our laboratory, which showed that 1A1, 1A7, 1A8, 1A9, and 1A10 were the major UGT isoforms to glucuronidate flavonoids. Also, certain UGT isoforms could produce sufficient amounts of regiospecific glucuronides of a flavonoid with multiple hydroxyl groups so that its online UV spectra will be of high quality (higher signal-to-noise ratio).

Thirty-six flavonoids belonging to the flavone or flavonol subclass with one or more hydroxyl and/or methoxyl substitutions at different positions were purchased from Indofine Chemicals (Somerville, NJ). The selected compounds consisted of 18 flavonoids with one hydroxyl group (i.e., 3-hydroxyflavone (or 3HF), 4′HF, 5HF, 6HF, 7HF, 3-hydroxy-4′-methoxyflavone (or 3H4′MF), 3H5MF, 3H6MF, 3H7MF, 4′H6MF, 4′H7MF, 5H7MF, 6H4′MF, 6H7MF, 7H4′MF, 5,7-dimethoxy-3-hydroxyflavone (or 5,7DM3HF), 6,4′DM3HF, 7,4′DM3HF); 13 flavonoids with two hydroxyl groups (i.e., 3,4′-dihydroxyflavone (or 3,4′DHF), 3,5DHF, 3,6DHF, 3,7DHF, 5,4′DHF, 5,6DHF, 5,7DHF, 6,4′DHF, 6,7DHF, 7,4′DHF, 5,4′-dihydroxy-7-methoxyflavone (or 5,4′DH7MF), 5,6DH7MF, 5,7DH8MF); 4 flavonoids with three hydroxyl groups (i.e., 3,6,4′-trihydroxyflavone (or 3,6,4′THF), galangin (or 3,5,7THF), resokaempferol (or 3,7,4′THF), and apigenin (or 5,7,4′THF)); and 1 flavonoid with four hydroxyl groups (i.e., kaempferol (or 3,5,7,4′-tetrahydroxyflavone)). All other materials (typically of analytical grade or better) were used as received.

Generation of Flavonoid Glucuronide(s) by UGTs. UGT 1A9 was used to generate most of the flavonoid glucuronides unless otherwise specified, and UGT 1A1 was used to generate glucuronides of 3,4′DHF, 3,6DHF, 3,7DHF, 5,6DHF, 6,4′DHF, 6,7DHF, 7,4′DHF, 3,6,4′THF, 5,6DH7MF, galangin, and resokaempferol. UGTs 1A7, 1A8, and 1A10 were additionally used for generating certain regiospecific glucuronides of kaempferol. Different UGTs were used for two reasons. First, these isoforms were able to generate enough metabolite of monohydroxyl flavonoid to produce good-quality UV spectra. Second, for certain multihydroxyl flavonoids, different UGT isoforms preferentially generate a regiospecific glucuronide in large quantities, allowing us to derive good UV spectra needed for position identification.

The incubation procedure producing glucuronides(s) was essentially the same as published previously (*18*, *28*). Briefly, incubation procedures using recombinant UGT isoforms (Supersomes) were as follows: (1) Supersomes (final concentration in the range of 0.0125−0.05 mg of protein/mL as optimum for the reaction, magnesium chloride (0.88 mM), saccharolactone (4.4 mM), alamethicin (0.022 mg/mL), 10 or 25 μM concentration of flavonoid in a 50 mM potassium phosphate buffer

(pH 7.4), and UDPGA (3.5 mM, add last)) were mixed; (2) the mixture (final volume = 200 μL) was incubated at 37 °C overnight so as to generate sufficient amounts of flavonoid glucuronides; and (3) the reaction was stopped by the addition of 50 μL of 94% acetonitrile/6% glacial acetic acid containing 50 μM internal standard. Testosterone was used as an internal standard for most compounds except 3,7DHF, for which 5-hydroxyflavone was used as internal standard, and 3HF, 3,5DHF, resokaempferol, and galangin, for which formononetin was used as an internal standard.

Generation of Online UV Spectra of Flavonoids and Their Glucuronides Using UPLC. The Waters Acquity UPLC (ultraperformance liquid chromatography) system equipped with a photodiode array detector (PDA), sample manager, binary solvent manager, Empower software, and BEH C_{18} column (1.7 μm, 2.1 × 50 mm) was used to separate each of the flavonoids and its glucuronides in the sample and obtain the corresponding UV spectra.

A general LC method was used for all of the analyses unless otherwise specified. The parameters used were as follows: mobile phase A, 100% aqueous buffer (2.5 mM ammonium acetate, pH 4.5); mobile phase B, 100% acetonitrile; flow rate, 0.45 mL/min; gradient, 0 min, 10% B, 0−2 min, 10−20% B, 2−3 min, 20−70% B, 3−3.5 min, 70% B, 3.5−4 min, 70−10% B; injection volume, 10 μL. For kaempferol, a different mobile phase A and gradient method were adopted: mobile phase A, 0.2% v/v formic acid; gradient, 0 min, 10% B, 0−2 min, 10−20% B, 2−3 min, 20−40% B, 3−3.5 min, 40−50% B, 3.5−4 min, 50−70% B, 4−4.5 min, 70% B, 4.5−5 min, 70−10% B. Kaempferol needed different conditions for better separation of the three glucuronides formed.

The absorbance values (*y*-axis scales) of UV spectral plots of each flavonoid and its metabolite(s) were normalized to the same dimensions with respect to each other using the normalization tool of the Empower software. The spectral plots of flavonoids and the corresponding metabolite(s) were displayed along the *y*-axis such that the axis range was 100% of the absorbance values range.

Confirmation of Glucuronides Using Hydrolysis with β-D-Glucuronidase. The glucuronidation reaction was run with UGT isoform(s) to almost complete substrate exhaustion at a substrate concentration of 25 μM. Glucuronides produced by UGT incubation were further purified using solid phase extraction. After a PolarPlus Octadecyl C_{18} Speedisk 10 μm solid phase extraction column (J. T. Baker; column volume, 3 mL) was washed with 2 mL of methanol and 1 mL of water, samples were loaded onto the column. One milliliter of water was then used to clear up the salts and saccharolactone, and successive 2 mL methanol elution fractions containing glucuronides were then collected. This was followed by 2 h of air-dying, and the residue was reconstituted with potassium phosphate butter (pH 7.4). A 500 μL portion of the metabolite solution was taken, and 415 units/mL β-D-glucuronidase was added to hydrolyze the metabolites (into aglycone) at 37 °C for 5 min. The control reaction was run using an equivalent volume of purified water in place of enzyme solution.

Confirmation of Degree of Substitution of Flavonoids Using UPLC/MS/MS. Glucuronides of flavonoids with more than one hydroxyl group in their structure were analyzed to confirm their degrees of glucuronic acid substitution (i.e., mono- or diglucuronides) using the UPLC/MS/MS method. Similar UPLC conditions as explained above were used to separate the flavonoids and their respective glucuronidess. The effluent from the Waters Acquity UPLC system was introduced into an API 3200 Qtrap triple-quadrupole mass spectrometer (Applied Biosystem/MDS SCIEX, Foster City, CA) mounted with a TurboIonSpray source. The working parameters for the mass spectrometers and compound-specific MS conditions were optimized. The mass of each individual peak of separated glucuronides was measured using QSMS mode. In MS^2 scan, precursor ion mode was used to confirm the identity of each peak as glucuronide, in which Q3 was held to measure the occurrence of the aglycone fragment ion and Q1 was scanned for the glucuronide ions that result in the corresponding aglycone ion (*29*, *30*).

RESULTS AND DISCUSSION

Generation and Confirmation of Flavonoids Glucuronide(s) by UGT Isoforms. Thirty-six selected flavones and flavonols with one or more hydroxyl groups at different positions (3, 5, 6, 7, or 4′) (**Figure 1**) in their structure were glucuronidated using either UGT 1A1, 1A7, 1A8, 1A9, or 1A10 isoforms. All flavonoids with one hydroxyl group formed single mono-*O*-glucuronides, regardless of the presence of the methoxyl group. Among flavonoids with two or more hydroxyl groups, 3,5DHF, 5,7DHF, 5,6DH7MF, 5,7DH8MF, and apigenin formed only one major detectable glucuronide, whereas 3,4′DHF, 3,6DHF, 3,7DHF, 5,4′DHF, 6,4′DHF, 7,4′DHF, and 5,4′DH7MF formed two major glucuronides and 3,6,4′THF, galangin, resokaempferol, and kaempferol formed three major glucuronides (Figure S2.33−S2.36 in the Supporting Information). Kaempferol formed kaempferol-3-*O*-glucuronide (or 3-*O*-G of kaempferol) and kaempferol-7-*O*-G (or 7-*O*-G of kaempferol) as the major metabolites and kaempferol-4′-*O*-G (or 4′-*O*-G of kaempferol) as the minor metabolite with the selected UGT isoforms.

The metabolite peaks were first confirmed as glucuronides by hydrolyzing them with β-D-glucuronidase as described in the method. All mono- or diglucuronide peaks disappeared to give respective aglycone peaks. **Figure 2A** showed the UPLC chromatograms of glucuronides of 3,4′DHF hydrolyzed with β-D-glucuronidase and their respective control samples. Similar results were obtained for other flavonoids and are shown in Figure S1A of the Supporting Information (SI). Galangin and kaempferol also showed one more mono-*O*-glucuronide most probably substituted at the 5-hydroxyl group, but the concentration was too low for proper UV spectrum analysis. Also, galangin and kaempferol formed a minor diglucuronide (confirmed by UPLC/MS/MS), but the UV spectrum shift method (i.e., change in λ_{max}) was unable to identify the positions of glucuronidation for galangin and kaempferol diglucuronides (Figure S1A, SI).

Confirmation of Degree of Substitution of Flavonoids by UPLC/MS/MS. Although treatment with glucuronidase was able to show that the metabolites were indeed glucuronides, the LC/MS/MS method was needed to show if the glucuronide was mono-, di-, or triglucuronide. The results indicated that glucuronidation of all selected flavonoids, even those with multiple hydroxyl groups, generated only one or more detectable mono-*O*-glucuronide(s) except for galangin and kaempferol, the glucuronidation of which also generated one diglucuronide each. Galangin diglucuronide was formed by UGTs 1A7 and 1A9 at 10 and 25 μM substrate concentrations, whereas kaempferol diglucuronide was formed by UGT 1A10 only at the highest concentration (25 μM).

Flavonoid mono- or diglucuronides were identified by MS and MS^2 (precursor ion) full-scan modes. The main working parameters for a few compounds for which mass spectrometry had been performed are shown in Table S1 of the Supporting Information. The conjugates produced strong mono-*O*-glucuronide molecular ions under the conditions used. **Figure 2B** shows MS scans of glucuronides of 3,4′DHF (m/z 431 $[M + 1]^+$) as examples. These diagnostic ions were also shown to form the respective aglycone by losing a glucuronic acid moiety (Figure S2B). Additionally, MS scans of glucuronides of 3HF (m/z 415 $[M + 1]^+$), 3,5DHF (m/z 431 $[M + 1]^+$), 3,7DHF (m/z 429 $[M - 1]^-$), galangin (m/z 445 $[M - 1]^-$), resokaempferol (m/z 445 $[M - 1]^-$), and kaempferol (m/z 461 $[M - 1]^-$) can be found in the Supporting Information (Figure S1B).

Confirmation of Position of Glucuronidation. The sites of mono-O-glucuronidation of flavonoids were determined on the basis of the λ_{max} shifts in their characteristic UV absorption spectra (*26*, *31*). **Figures 3−6** show the UV spectra of 16 selected flavonoids and their corresponding single mono-*O*-glucuronides at 3-, 7-, 4′-, or 5-positions as examples, and others were more or less similar (see Figure S2 of the SI). A systematic analysis of UV spectrum change as the result of glucuronidation of 18 different

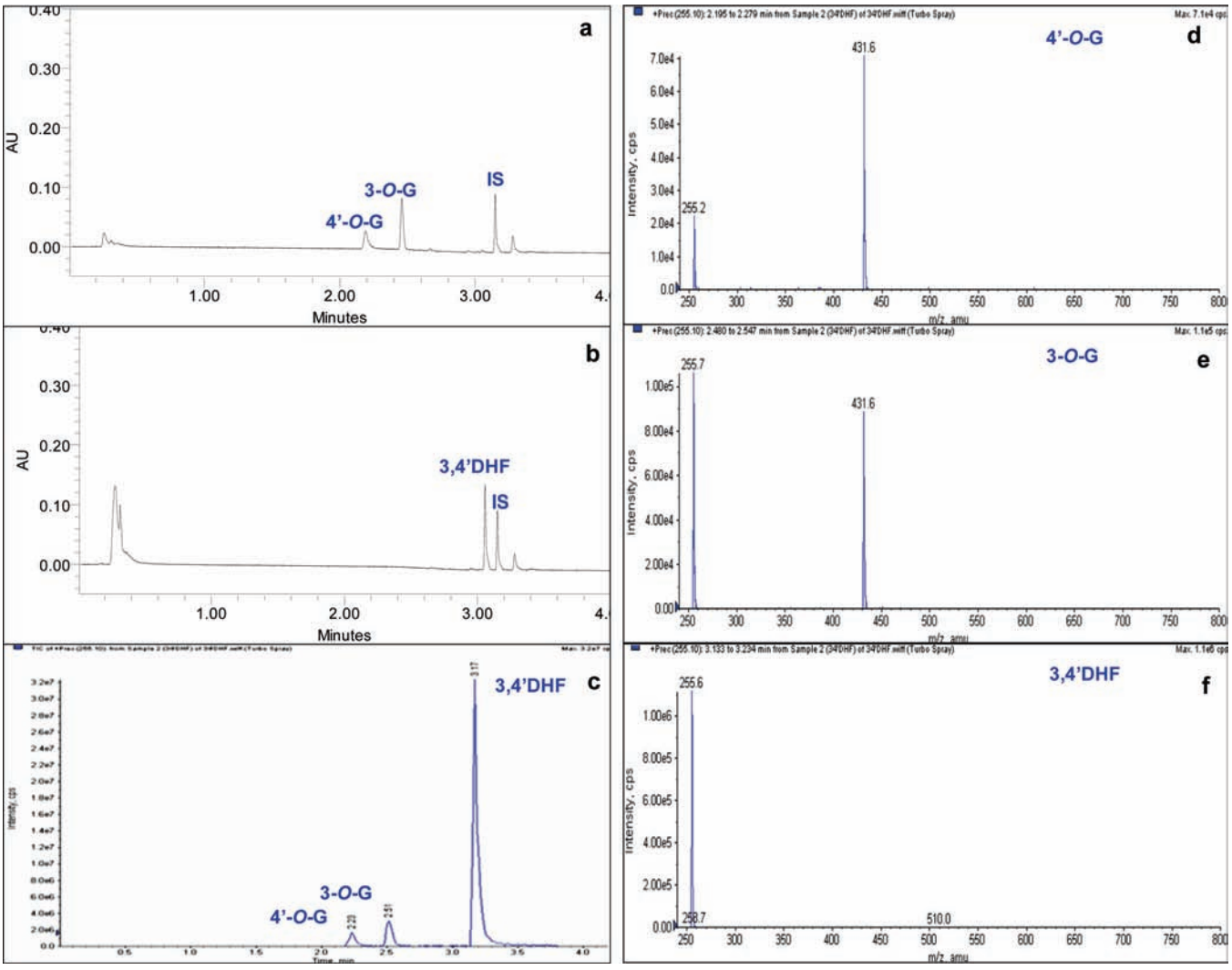

Figure 2. (**A**) UPLC chromatograms at 254 nm of (top, control sample; bottom, sample after hydrolysis with β-D-glucuronidase); (**B**) LC/MS/MS scans of 3,4′DHF and its glucuronides generated by UGT 1A1 at an incubation concentration of 25 μM.

flavonoids with one hydroxyl group at 3, 4′, 5, 6, or 7 showed how λ_{max} shifted due to glucuronidation (Figure S2.1−S2.18 of the SI), which are detailed below.

The analysis demonstrated how positions of glucuronidation of 18 flavonoids (with more than one hydroxyl groups) were solved on the basis of changes in λ_{max} value or spectrum shift obtained from glucuronidation of 18 flavonoids with only one hydroxyl group. To simplify the data presentation, results are organized according to the position of glucuronidation of the hydroxyl group in the flavonoid structure.

In cases when there were more than one mono-*O*-glucuronide, we were able to identify each of mono-*O*-glucuronide by identifying either the maximal number of mono-*O*-glucuronides possible (i.e., three mono-*O*-glucuronide for a trihydroxyflavone) or by eliminating the 5-OH group as a group for glucuronidation in flavonoid with multiple hydroxyl groups because 5-O-glucuronidaton was very slow and generally not detectable under current reaction conditions.

Effects of Glucuronidation at the 3-Hydroxyl Group on λ_{max} Shift in UV Spectra. The resulting UV spectra showed that the glucuronidation of the hydroxyl position at C_3 resulted in either diminishment of UV absorption or an approximately 14−29 nm hypsochromic shift in band I λ_{max}, but no consistent shift in band II λ_{max} (Figure S2.1−S2.8, SI). The results are shown in **Table 1**. As examples, shifts in band I and band II λ_{max} of 3-*O*-glucuronide of 3HF, 3H5MF, 3,5DHF, and resokaempferol (3,7,4′THF) are shown in **Figure 3**.

All flavonoids with a 3-hydroxyl group alone or with one or more hydroxyl group(s) at other position(s) were shown to form at least one 3-*O*-glucuronide with a hypsochromic shift in band I λ_{max} in the above-mentioned range. For example, glucuronidation of the 3-hydroxyl group of 3HF causes the disappearance of band I in the UV spectra of 3-*O*-glucuronide of 3HF (**Figure 3a**). 3-O-Glucuronidation of 3H5M, 3,5DHF, and respokaempferol caused hyposchromic band I λ_{max} shifts of 18.9, 13.3, and 14.3 nm, respectively (**Figure 3b−d**). **Table 1** shows a diagnostic hypsochromic shift in band I λ_{max} of the UV spectra of 3-*O*-glucuronides of 16 flavonols.

Detailed spectral data (corresponding to values in **Table 1**) are shown in Figures S3 (a−d), S2.19−S2.22, S2.33−S2.36 of the Supporting Information. The λ_{max} shift of unknown flavonoid (those with more than one hydroxyl group) glucuronides was predicted correctly on the basis of the shifts in λ_{max} of the known flavonoid with only one hydroxyl group to form 3-*O*-glucuronides.

The prediction was made easy because all 3-*O*-glucuronides showed band I λ_{max} hyposchromic shifts within the range of ~14−29 nm. The smallest band I λ_{max} shift (13.3 nm) was displayed by 3-*O*-glucuronide of 3,5DHF. This strongly suggested that a band I λ_{max} hypsochromic shift of an unknown

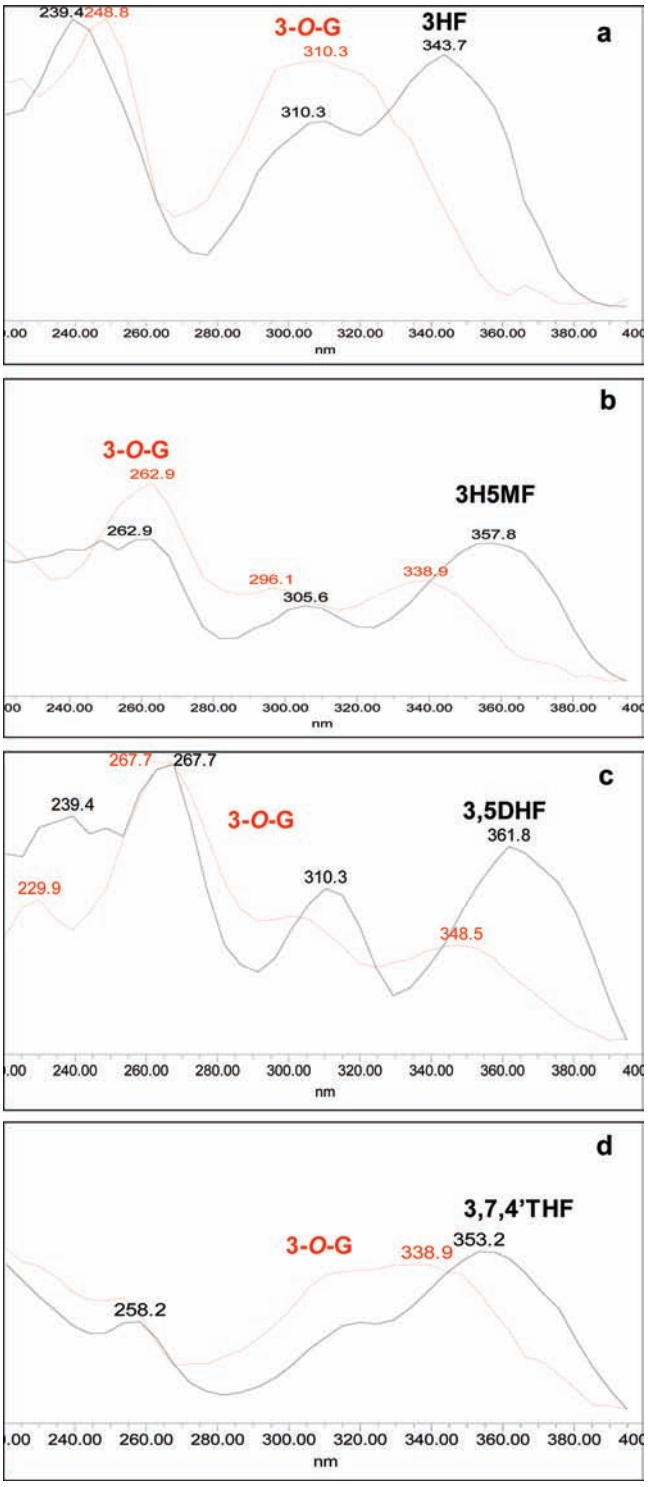

Figure 3. UV spectra of (**a**) 3HF, (**b**) 3H5M, (**c**) 3,5DHF, and (**d**) resokaempferol (3,7,4′THF) (solid black line) and their 3-*O*-glucuronides (red dotted line) generated by either UGT 1A1, 1A7, 1A8, 1A9, or 1A10 at an incubation concentration of 10 or 25 μM.

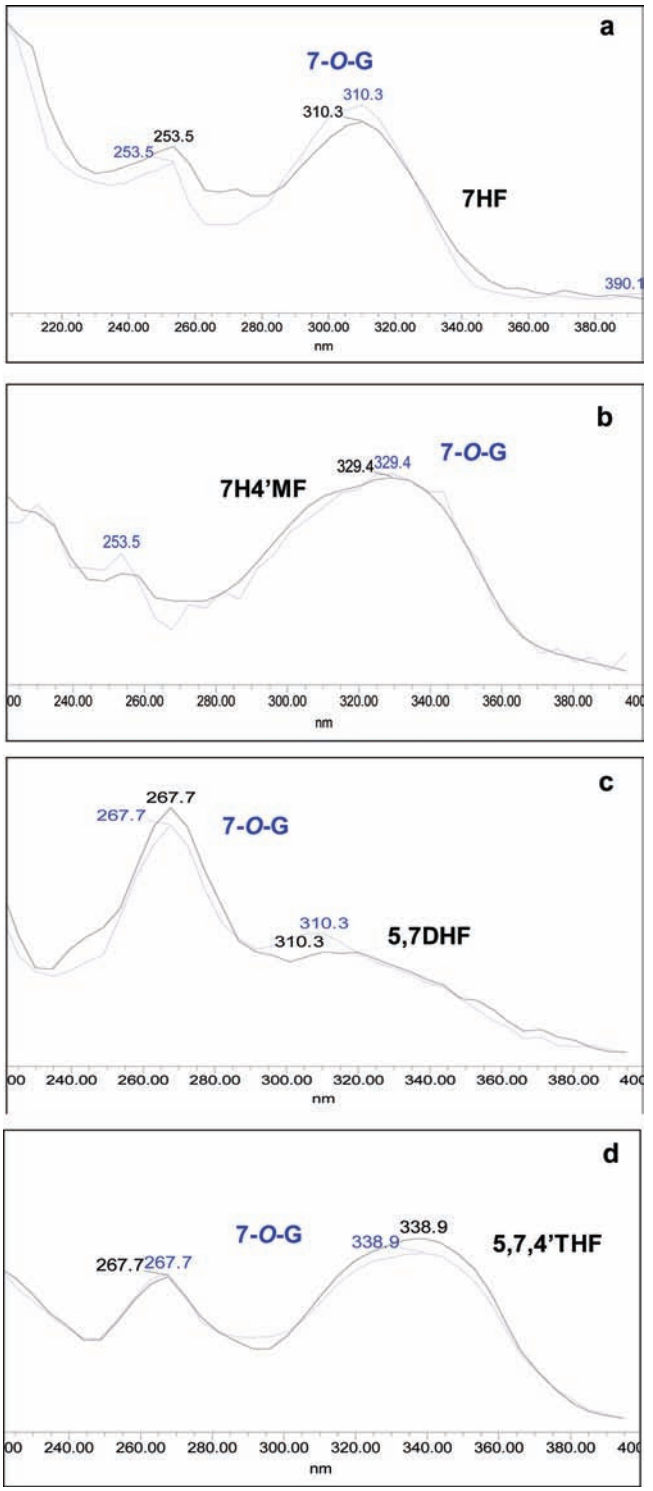

Figure 4. UV spectra of (**a**) 7HF, (**b**) 7H4′M, (**c**) 5,7DHF, and (**d**) apigenin (5,7,4′THF) (solid black line) and their 7-*O*-glucuronides (blue dotted line) generated by either UGT 1A1, 1A7, 1A8, 1A9, or 1A10 at an incubation concentration of 10 or 25 μM.

flavonol glucuronide in the range of ~13−30 nm without a corresponding shift in band II λ_{max} value could be used as a spectrum tool to determine the position of glucuronidation of flavonols (or flavones with a 3-hydroxyl group).

Effects of Glucuronidation at the 7-Hydroxyl Position on λ_{max} Shift in UV Spectra. The glucuronidation of the 7-hydroxyl group had no or minimal effect on the band I or band II λ_{max} values in the UV spectrum of 11 flavonoid glucuronides (**Figure 4a**,**b**). UV spectra of 7HF, 7H4′M, 5,7DHF, and apigenin (5,7,4′THF) and their respective 7-*O*-glucuronides are shown in **Figure 4** as examples. All selected flavonoids with a free hydroxyl group at C_7 formed a 7-*O*-glucuronide. None of the formed 7-*O*-glucuronides showed any change in their spectra or λ_{max} values except for the 7-*O*-glucuronide of 3,7DHF, which showed a hyposchromic shift of −4.7 nm in band II λ_{max} (**Table 2**).

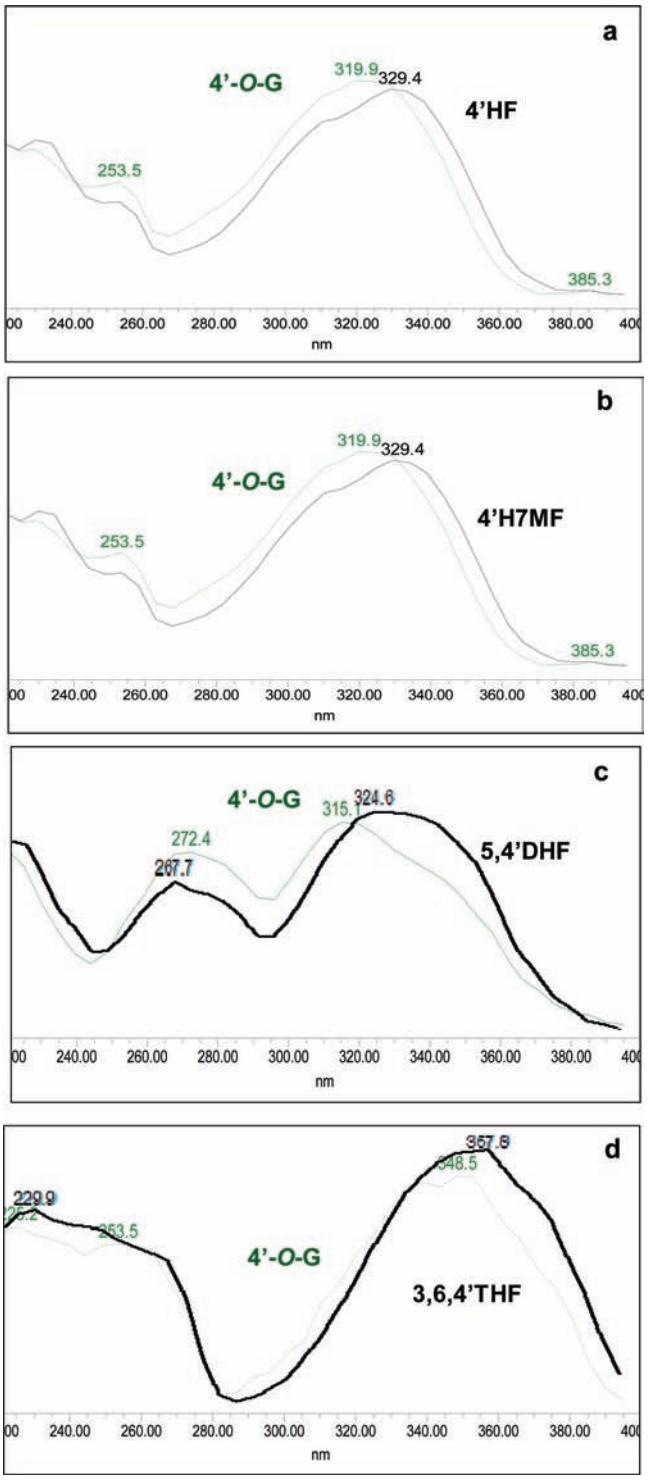

Figure 5. UV spectra of (**a**) 4′HF, (**b**) 4′H7M, (**c**) 5,4′DHF, and (**d**) 3,6,4′THF (solid black line) and their 4′-*O*-glucuronides (green dotted line) generated by either UGT 1A1, 1A7, 1A8, 1A9, or 1A10 at an incubation concentration of 10 or 25 μM.

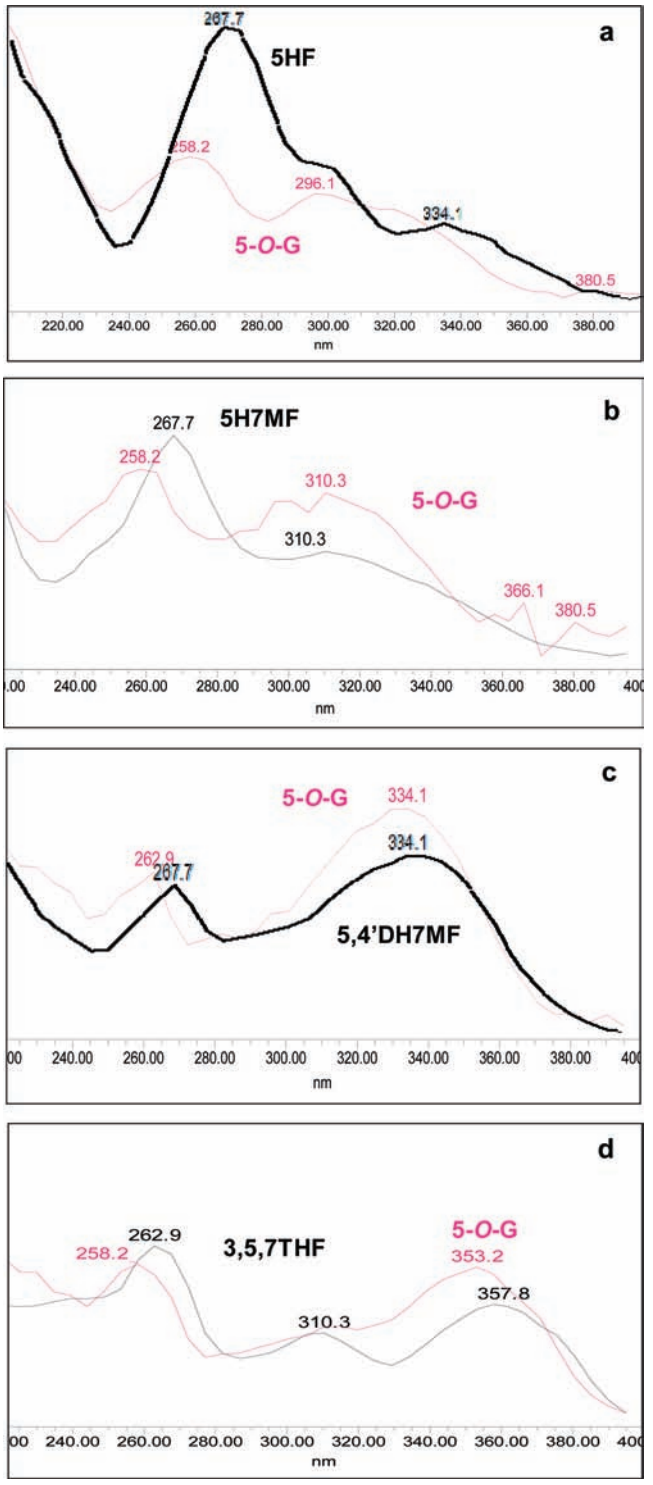

Figure 6. UV spectra of (**a**) 5HF, (**b**) 5H7M, (**c**) 5,4′DH7MF, and (**d**) galangin (3,5,7THF) (solid black line) and their 5-*O*-glucuronides (magenta dotted line) generated by either UGT 1A1, 1A7, 1A8, 1A9, or 1A10 at an incubation concentration of 10 or 25 μM.

In the case of 3,7DHF, one glucuronide showed a hypsochromic shift of ~23.8 nm in band I λ_{max} with no shift in band II λ_{max}, whereas the other showed a hyposchromic shift of −4.7 nm in band II λ_{max} but no change in band I (Figure S2.22, SI). These results indicated that the one glucuronide with a shift of ~23.8 nm in band I λ_{max} was glucuronidated at the 3-hydroxyl group, whereas the other one was glucuronidated at the 7-hydroxyl group. Similarly, 5,7DHF formed only one glucuronide (**Figure 4c**), which did not show any change in UV scan, confirming that the 7-hydroxyl group was glucuronidated in this case.

In cases of both 6,7DHF (Figure S2.27, SI) and 7,4′DHF (Figure S2.28, SI), one glucuronide showed no shift at all, whereas the other showed a hypsochromic shift of ~10 nm in band I λ_{max}, suggesting that the one with no shift in λ_{max} was glucuronidated at the 7-hydroxyl group and the other was glucuronidated at the

Table 1. Diagnostic Shifts in Band I of the 3-*O*-Glucuronides in Relation to the Corresponding Aglycone

		λ_{max} (nm)			
compound	aglycone or glucuronide (*O*-G)	band II	band I	diagnostic shift in band I in relation to aglycone	Figure number in SI
3HF	aglycone	239.4	343.7		2.1
	3-O-G	248.8		band I disappeared	2.1
3H4′MF	aglycone	234.7	353.2		2.2
	3-O-G	ND[a]	329.4	−23.8 nm	2.2
3H5MF	aglycone	262.9	357.8		2.3
	3-O-G	262.9	338.9	−18.9 nm	2.3
3H6MF	aglycone	253.5	329.4		2.4
	3-O-G	262.9	310.2	−19.1 nm	2.4
3H7MF	aglycone	253.5	338.9		2.5
	3-O-G	248.8	310.3	−28.6 nm	2.5
5,7DM3H	aglycone	253.5	348.5		2.6
	3-O-G	ND	329.4	−19.1 nm	2.6
6,4′DM3HF	aglycone	ND	348.5		2.7
	3-O-G	ND	334.1	−14.4 nm	2.7
7,4′DM3HF	aglycone	262.9	348.5		2.8
	3-O-G	262.9	329.4	−19.1 nm	2.8
3,4′DHF	aglycone	234.7	357.8		2.19
	3-O-G	234.7	329.4	−28.4 nm	2.19
3,5DHF	aglycone	267.7	361.8		2.20
	3-O-G	267.7	348.5	−13.3 nm	2.20
3,6DHF	aglycone	258.2	329.4		2.21
	3-O-G	253.5	315.1	−14.3 nm	2.21
3,7DHF	aglycone	253.5	338.9		2.22
	3-O-G	248.8	315.1	−23.8 nm	2.22
galangin	aglycone	262.9	357.8		2.33
	3-O-G	262.9		band I disappeared	2.33
3,6,4′THF	aglycone	ND	357.8		2.34
	3-O-G	267.7	338.9	−18.9 nm	2.34
resokaempferol	aglycone	253.5	353.2		2.35
	3-O-G	ND	338.9	−14.3 nm	2.35
kaempferol	aglycone	262.9	366.1		2.36
	3-O-G	262.9	348.5	−17.6 nm	2.36

[a] ND, not detected by the Empower software in the spectra.

4′- or 6-hydroxyl group, respectively. How glucuronidation at the 4′- and 6′-hydroxyl groups affected UV spectra will be discussed below in their respective sections.

Glucuronidation of apigenin (**Figure 4d**), galangin (Figure S2.33, SI), resokaempferol (Figure S2.35, SI), and kaempferol (Figure S2.36, SI) at the 7-*O* position also did not change their respective UV spectra. On this basis, we deduced that in most cases (perhaps with rare exceptions not found here), no change in UV spectra of an unknown flavone/flavonol glucuronide was diagnostic of the fact that the position of glucuronidation was the 7-hydroxyl group.

Table 2. Diagnostic Shifts in Bands I and II of the 7-*O*-Glucuronides in Relation to the Corresponding Aglycone

		λ_{max} (nm)			
compound	aglycone or glucuronide (*O*-G)	band II	band I	diagnostic shifts in bands I and II in relation to aglycones	Figure number in SI
7HF	aglycone	253.5	310.3		2.17
	7-O-G	253.5	310.3	no change	2.17
7H4′MF	aglycone	ND[a]	329.4		2.18
	7-O-G	ND	329.4	no change	2.18
3,7DHF	aglycone	253.5	338.9		2.22
	7-O-G	248.8	338.9	no change (band I) −4.7 nm (band II)	2.22
5,7DHF	aglycone	267.7	310.3		2.25
	7-O-G	267.7	310.3	bo change	2.25
6,7DHF	aglycone	267.7	319.9		2.27
	7-O-G	267.7	319.9	no change	2.27
7,4′DHF	aglycone	ND	334.1		2.28
	7-O-G	253.5	334.1	no change	2.28
5,7DH8MF	aglycone	272.4	343.7		2.31
	7-O-G	272.4	343.7	no change	2.31
apigenin	aglycone	267.7	338.9		2.32
	7-O-G	267.7	338.9	no change	2.32
galangin	aglycone	262.9	357.8		2.33
	7-O-G	262.9	357.8	no change	2.33
resokaempferol	aglycone	253.5	353.2		2.35
	7-O-G	253.5	353.2	no change	2.35
kaempferol	aglycone	262.9	366.1		2.36
	7-O-G	262.9	366.1	no change	2.36

[a] ND, not detected by the Empower software in the spectra.

Effects of Glucuronidation at the 4′-Hydroxyl Group on λ_{max} Shift in UV Spectra. Glucuronidation of the 4′-hydroxyl group resulted in an approximately 4−10 nm hypsochromic shift in band I λ_{max} but inconsistent shift in band II λ_{max} (Figure S2.9−S2.11, SI). The results are shown in **Table 3**. UV spectra of 4′HF, 4′H7M, 5,4′DHF, and 3,6,4′THF and their respective 4′-*O*-glucuronides are shown in **Figure 5**, as examples.

In the case of 3,4′DHF, one glucuronide showed a hypsochromic shift of ∼28.4 nm in band I λ_{max}, whereas the other showed a shift of only ∼5 nm in band I λ_{max} with no shift in band II λ_{max} (Figure S2.19, SI). These results indicated that the glucuronide with a ∼28.4 nm shift in band I λ_{max} was glucuronidated at the 3-hydroxyl group, whereas the other was glucuronidated at the 4′-hydroxyl group. This was consistent with the information obtained from the glucuronidation of known 3- and 4′-hydroxyl groups (**Table 3**).

Similarly, the 7-*O*-glucuronide of 7,4′DHF showed no spectrum shift at all, whereas the 4′-*O*-glucuronide of 7,4′DHF showed a hypsochromic shift of ∼9.5 nm in band I λ_{max} (Figure S2.28, SI), consistent with the information obtained from spectra shift of known 4′-*O*-glucuronides. Also, the 4′-*O*-glucuronides of resokaempferol (Figure S2.35, SI) and kaempferol (Figure S2.36, SI) showed hypsochromic shifts of ∼4.7 and 8.3 nm in band I λ_{max}, respectively (**Table 3**). Because the 3-*O*-glucuronide and 7-*O*-glucuronide of these tetra-hydroxyl flavonoids

Table 3. Diagnostic Shift in Band I of the 4′-*O*-Glucuronides in Relation to the Corresponding Aglycone

compound	aglycone or glucuronide (*O*-G)	λ_{max} (nm) band II	λ_{max} (nm) band I	diagnostic shifts in band I in relation to aglycones	Figure number in SI
4′HF	aglycone	253.5	324.6		2.9
	4′-O-G	248.8	315.1	−9.5 nm	2.9
4′H6MF	aglycone	272.4	329.4		2.10
	4′-O-G	272.4	324.6	−4.8 nm	2.10
4′H7MF	aglycone	ND[a]	329.4		2.11
	4′-O-G	253.5	319.9	−9.5 nm	2.11
3,4′DHF	aglycone	234.7	357.8		2.19
	4′-O-G	ND	353.2	−4.6 nm	2.19
5,4′DHF	aglycone	267.7	329.4		2.23
	4′-O-G	272.4	315.1	−9.5 nm	2.23
6,4′DHF	aglycone	272.4	329.4		2.26
	4′-O-G	272.4	319.9	−9.5 nm	2.26
7,4′DHF	aglycone	253.5	334.1		2.28
	4′-O-G	253.5	324.6	−9.5 nm	2.28
5,4′DH7MF	aglycone	267.7	338.9		2.29
	4′-O-G	267.7	324.6	−9.5 nm	2.29
3,6,4′THF	aglycone	ND	357.8		2.34
	4′-O-G	258.2	348.5	−9.3 nm	2.34
resokaempferol	aglycone	253.5	353.2		2.35
	4′-O-G	253.5	348.5	−4.7 nm	2.35
kaempferol	aglycone	262.9	366.1		2.36
	4′-O-G	262.9	357.8	−8.3 nm	2.36

[a] ND, not detected by the Empower software in the spectra.

were easily recognized as shown earlier, it was possible to identify the 4′-*O*-glucuronides of these two compounds by rule of elimination also.

On the basis of the above observations, we determined the 4′-*O*-glucuronides of 5,4′DHF (**Figure 5c**), 6,4′DHF (Figure S2.26, SI), 3,6,4′THF (**Figure 5d**), and 5,4′DH7MF (Figure S2.29, SI), all of which showed a hypsochromic shift of about ∼9.5 nm in band I λ_{max} (**Table 3**). Therefore, we deduced that glucuronidation at the 4′-hydroxyl group would show a consistent and diagnostic hypsochromic shift in band I λ_{max} in the range of 4−10 nm.

Effects of Glucuronidation at the 5-Hydroxyl Group on λ_{max} Shift in UV Spectra. Glucuronidation of the 5-hydroxyl group could cause a hypsochromic shift of ∼10 nm in band II λ_{max} (**Figure 6**), whereas no consistent shifts in λ_{max} of band I could be observed (Figure S2.12−S2.13, SI), as shown in **Table 4**. Among the selected multihydroxyl flavonoids, there were nine flavonoids with a free 5-hydroxyl group, but only four flavonoids (or about 44%) formed 5-*O*-glucuronide in detectable amounts, strongly suggesting that in the presence of additional hydroxyl groups, the 5-hydroxyl group was not the favored position of O-glucuronidation.

In the case of 5,4′DHF (**Figure 6c**), 5,4′DH7MF (Figure S2.29, SI), and galangin (3,5,7THF) (**Figure 6d**), the UV spectra of 5-*O*-glucuronides showed a hypsochromic shift of only ∼5 nm in band II λ_{max}. However, in both cases, 5-*O*-glucuronides could also be deduced on the basis of the rule of elimination, suggesting that

Table 4. Diagnostic Shift in Band II of the 5-*O*-Glucuronides in Relation to the Corresponding Aglycone

compound	aglycone or glucuronide (*O*-G)	λ_{max} (nm) band II	λ_{max} (nm) band I	diagnostic shifts in band II in relation to aglycones	Figure number in SI
5HF	aglycone	267.7	334.1		2.12
	5-O-G	258.2	324.1	−9.5 nm	2.12
5H7MF	aglycone	267.7	310.3		2.13
	5-O-G	258.2	310.3	−9.5 nm	2.13
5,4′DHF	aglycone	267.7	329.4		2.23
	5-O-G	262.9	334.1	−4.8 nm	2.23
5,6DHF	aglycone	281.9	ND[a]		2.24
	5-O-G	272.4	310.3	−9.5 nm	2.24
5,4′DH7MF	aglycone	267.7	338.9		2.29
	5-O-G	258.2	334.1	−4.8 nm	2.29
galangin	aglycone	262.9	357.8		2.33
	5-O-G	258.2	353.2	−4.7 nm	2.33

[a] ND, not detected by the Empower software in the spectra.

glucuronidation of the 5-hydroxy group could also cause a hypsochromic shift in range of ∼5 nm, whereas the UV spectra of the 5-*O*-glucuronide of 5,6DHF (Figure S2.24, SI) showed a hypsochromic shift of ∼9.5 nm in band II λ_{max}, which conformed to the UV spectra of glucuronides of 5HF and 5H7MF. On this basis, we deduced that glucuronidation at the 5-hydroxyl group would show a consistent and diagnostic hypsochromic shift in band II λ_{max} in the range of 4−10 nm.

Effect of Glucuronidation at the 6-Hydroxyl Group on λ_{max} Shift in UV Spectra. The glucuronidation of the 6-hydroxyl group can cause either no change or random change in band I and/or II λ_{max} values (Figure S2.14−S2.16, SI). Therefore, in most cases glucuronidation at the 6-hydroxyl group was determined by rule of elimination. The results showed that as compared to diagnostic spectral shift for other glucuronides, 6-*O*-glucuronides did not have any consistent shift in either band I or band II λ_{max}. Results obtained by the rule of elimination are shown in **Table 5**.

Glucuronidation at the 6-OH position did not produce any consistent λ_{max} shift. Moreover, 5-O-glucuronidation did not show a consistent shift in band I, whereas 4′-O-glucuronidation did not show a consistent shift in band II. This might pose a difficulty in the identification of the position of glucuronidation in the flavonoids where these groups occur together. To solve this, the amount of different mono-*O*-glucuronides formed in the mixture could also be used as additional information. In general, the rank of preference for the position of glucuronidation was found to be 6-*O*-G > 4′-*O*-G > 5-*O*-G, such that in any of the tested compounds, 5-*O*-G was the least formed glucuronide. Therefore, for mono-*O*-glucuronides for which diagnostic shifts in λ_{max} do not provide clear and sufficient information, relative rates of mono-*O*-glucuronide formation can be helpful in the identification of position of glucuronidation. Because the relative rates of formation would depend on the organism and enzyme isoforms used, only the relative rates of formation of different mono-*O*-glucuronides of a flavonol/flavone by a standardized enzymatic system such as commercially available human recombinant UGT isoforms could be used as diagnostics for comparison.

Challenges of Using λ_{max} Shift in UV Spectra To Determine the Regiospecific Glucuronide. For certain flavonoids that had

Table 5. Diagnostic Shift in Bands I and II of the 6-*O*-Glucuronides in Relation to the Corresponding Aglycone

		λ_{max} (nm)			
compound	aglycone or glucuronide (*O*-G)	band II	band I	diagnostic shifts in bands I and II in relation to aglycones	Figure number in SI
6HF	aglycone	267.7	305.6		2.14
	6-O-G	262.9	305.6	no change (band I) −4.8 nm (band II)	2.14
6H4′MF	aglycone	277.1	310.3		2.15
	6-O-G	277.1	310.3	no change (band I) no change (band II)	2.15
6H7MF	aglycone	262.9	305.6		2.16
	6-O-G	262.9	310.3	+4.7 nm (band I) no change (Band II)	2.16
3,6DHF	aglycone	258.2	329.4		2.21
	6-O-G	253.5	329.4	no change (band I) −4.7 nm (band II)	2.21
5,6DHF	aglycone	281.9	ND[a]		2.24
	6-O-G	277.1	ND	−4.8 nm (band II)	2.24
6,4′DHF	aglycone	272.4	329.4		2.26
	6-O-G	267.7	329.4	no change (band I) −4.7 nm (band II)	2.26
6,7DHF	aglycone	267.7	319.9		2.27
	6-O-G	267.7	310.3	−9.6 nm (band I) no change (band II)	2.27
5,6DH7MF	aglycone	277.1	319.9		2.30
	6-O-G	272.4	319.9	no change (band I) −4.7 nm (band II)	2.30
3,6,4′THF	aglycone	ND	357.8		2.34
	6-O-G	ND	353.2	−4.6 nm (band I)	2.34

[a] ND, not detected by the Empower software in the spectra.

hydroxyl groups only in ring A but not in the ring B or C in their structures (e.g., 5,7-DHF), if one diagnostic band did not show a very high peak in the UV spectra in relation to the other diagnostic band (at least ~20%), the smaller band was not always reliable for determining the diagnostic shifts in λ_{max}. In this case, relative formation rates of different regiospecific glucuronides (e.g., 6-*O*-G > 4′-*O*-G > 5-*O*-G) would be helpful (see **Table 6**).

The λ_{max} values of bands I and II in the UV spectra of the flavones and flavonols and their respective mono-*O*-glucuronides at different positions were somewhat dependent (within a few nanometers) on the chromatographic conditions used such as pH of mobile phases, solvent used, and gradient speed. However, none of the selected flavonoids showed any deviation from the conclusion made in this paper in that the diagnostic λ_{max} shift values stayed relatively constant (within the range).

The elution order of the regiospecific mono-*O*-glucuronides could have been used to identify the specific metabolite. However, the elution order was shown to change randomly with the chromatographic conditions used as well as with the positions of free hydroxyl groups in the structure of flavonoids, and there was no specific order pattern that can be used to identify the position of glucuronidation (as shown in Figure S1A, SI).

Use of Spectral λ_{max} Shift Method To Identify Mono-*O*-glucuronides of Quercetin. We used human recombinant UGT 1A9 and UGT 1A10 to generate the four mono-*O*-glucuronides of quercetin. The UV λ_{max} shift of bands I and II of the four mono-*O*-glucuronides with retention times are shown in **Table 7**. UGT 1A9 formed glucuronides I, II, and IV, whereas UGT 1A10 formed glucuronides I, II, and III. On the basis of the diagnostic shift in λ_{max} of bands I and II of the four mono-*O*-glucuronides of quercetin (**Figure 7**), we were able to identify glucuronide II and glucuronide III as 3-*O*-G and 4′-*O*-G, respectively (**Table 7**). However, it was difficult to identify the position of glucuronidation of glucuronides I and IV, which generated almost similar λ_{max} shift patterns. On the basis of the published literature on the elution order (*20*, *25*, *32*, *33*) of quercetin glucuronides, we could identify glucuronide I and glucuronide IV as 7-*O*-G and 3′-*O*-G, respectively.

Additional supporting evidence for the identification of glucuronide I and glucuronide IV as 7-*O*-G and 3′-*O*-G, respectively, was provided by the rates of formation of these quercetin glucuronides by UGTs. In our study, UGT 1A9 formed 7-*O*-G, 3-*O*-G, and 3′-*O*-G at 1.29 ± 0.21, 1.43 ± 0.23, and 0.7 ± 0.09 nmol/min/mg, respectively. UGT 1A10 formed 7-*O*-G, 3-*O*-G, and 4′-*O*-G at 0.8 ± 0.06, 0.57 ± 0.09, and 0.33 ± 0.12 nmol/min/mg, respectively. This was consistent with the published reports on the formation of quercetin glucuronides by human liver, intestine, and UGT isoforms (*32*, *34*). This suggested that the available information in the literature on the rates of formation of glucuronides and elution order of the mono-*O*-glucuronides of particular flavonoid could also be useful in identifying the position of glucuronidation. However, if such information is unavailable, it would be very difficult to differentiate between glucuronidation at position 3′-*O* and that at position 7-*O*.

Table 6. Effect of Regiospecific Glucuronidation on the λ_{max} of Bands I and II in the UV Spectra of Flavones and Flavonols

	effect on λ_{max}	
position of glucuronidation	band I	band II
3-*O*	~13−30 nm hypsochromic shift in λ_{max}	no consistent shift in λ_{max}
7-*O*	no change in λ_{max}	no change in λ_{max}
4′-*O*	~4−10 nm hypsochromic shift in λ_{max}	no consistent shift in λ_{max}
5-*O*	no consistent shift in λ_{max}	~4−10 nm hypsochromic shift in λ_{max}
6-*O*	no consistent shift in λ_{max}	no consistent shift in λ_{max}

Table 7. Diagnostic Shift in Bands I and II of the Mono-*O*-glucuronides of Quercetin in Relation to Quercetin

	λ_{max} (nm)			
compound/glucuronide (retention time) (color of line in **Figure 7**)	band II	band I	diagnostic shifts in bands I and II	position of O-glucuronidation
quercetin (2.87 min) (black solid)	255.7	373.6		
glucuronide I (1.04 min) (red dotted)	255.7	371.2	−2.4 nm (band I) no change (band II)	7-*O*-G
glucuronide II (1.25 min) (blue dashed)	258.2	356.2	−17.4 nm (band I) +2.5 nm (band II)	3-*O*-G
glucuronide III (1.47 min) (green dotted dashed)	253.3	366.2	−7.4 nm (band I) −2.4 nm (band II)	4′-*O*-G
glucuronide-IV (1.80 min) (brown double-dotted dashed)	253.3	371.2	−2.4 nm (band I) −2.4 nm (band II)	3′-*O*-G

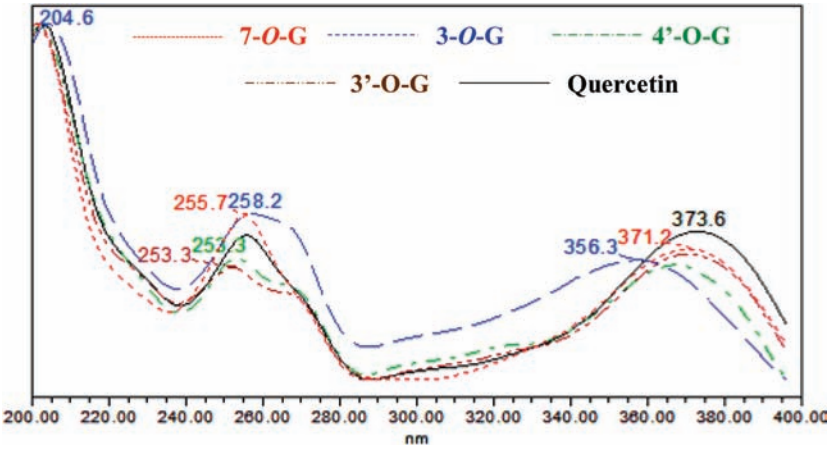

Figure 7. UV spectra of quercetin (3,5,7,3′,4′-pentahydroxyflavone) (solid black line) and its four mono-*O*-glucuronides generated by UGT 1A8 and UGT 1A9 at an incubation concentration of 10 μM.

Possible Application of the Spectrum λ_{max} Shift Method. The newly established method of identifying the position of glucuronidation will enable multiple areas of research: glucuronidation reaction including isoform-specific glucuronidation and structure−metabolism relationship, glucuronide transport, and/or UGT polymorphism. This method could also be used to give more precise structural information about flavonoid glucuronides, which is a significant improvement as most of the papers published regarding flavonoid glucuronidation were not able to pinpoint the position of the glucuronide group.

Isoform-specific glucuronidation is closely related to the regiospecific glucuronidation of flavonoids by various UGT isoforms. Therefore, identification of the glucuronide position could facilitate the determination of whether a specific UGT isoform prefers a particular hydroxyl position. For example, in the case of 3,4′DHF, UGT 1A9 glucuronidated only the 3-hydroxyl group, whereas UGT 1A1 glucuronidated both 3- and 4′-hydroxyl groups. On the other hand, UGT 1A9 did not glucuronidate the 4′-hydroxyl group in resokaempferol (3,7,4′THF), but UGT 1A1 was able to metabolize all three hydroxyl groups. This suggested that the 4′-position was not a favored position of glucuronidation by UGT 1A9, although the same group was not unfavored by UGT 1A1. Assuming that glucuronidation of a hydroxyl group in a particular flavonoid is exclusively favored by one particular UGT isoform, the specific glucuronide level might be used as a diagnostic tool to determine the expression levels of a specific isoform in vivo.

Second, the identification of position of glucuronidation of a compound could also help us understand the relationship between the structure of glucuronides and their transport by efflux transporter. Jeong et al. showed that total (apical and basolateral) excretion rates of the raloxifene-4′-*O*-glucuronide from the Caco-2 cell monolayer and the rates of its formation in the cell lysate

were ~7.6 and ~2.2 pmol/min/monolayer, respectively. In other words, the excretion rates of the raloxifene-4′-*O*-glucuronide from the Caco-2 cells monolayer were 3.4 times higher than the rate of its formation in the cell lysate (*35*). This suggested that the efflux transporter(s) involved was (were) favoring the excretion of raloxifene-4′-*O*-glucuronide from the cell such that the glucuronidation reaction was favored in the forward direction.

Recent data from our laboratory also showed that the rates of formation of the two mono-*O*-glucuronides of 3,7DHF, 3-*O*-glucuronide and 7-*O*-glucuronide in Caco-2 cell lysate were 19.27 ± 1.9 and 4.75 ± 1.7 nmol/h/mg of protein (4-fold difference), respectively, whereas the rates of total excretion of 3-*O*-glucuronide and 7-*O*-glucuronide of 3,7DHF in Caco-2 cell monolayer were 0.75 ± 0.03 and 0.66 ± 0.03 nmol/h/mg of protein (1.1-fold difference), respectively. Both examples discussed above suggested that the excretion of flavonoid glucuronides in an organ or cell line was not only decided by the activities of UGT isoforms but also influenced by the activities of responsible efflux transporter(s).

Third, knowledge of the preference of position to be glucuronidated in the flavonoid structure and excretion of glucuronides could also be used to generate the in silico quantitative structure−activity relationship models for UGTs and various efflux transporters such as MRP2 and BCRP. Smith et al. used mapping of glucuronidation sites as one of the features to generate common-feature pharmacophores of UGT 1A4 (*36*). Also, Williamson et al. used interaction of quercetin glucuronides, 3-*O*-β-D-glucuronide, 7-*O*-β-D-glucuronide, 3′-*O*-β-D-glucuronide, and 4′-*O*-β-D-glucuronide, with MRP2 to assess the predictive power of an in silico generated three-dimensional homology model of MRP2 (*37*).

This technique could be successfully utilized for the identification of position of glucuronidation in the samples generated in different experimental matrix including in vitro samples such as microsomal samples and in vivo samples such as plasma. It is, however, important that samples should be reasonably cleaned using solid or liquid phase extraction such that the experimental matrix does not interfere with UV spectra. Also, a sufficient quantity of analyte should be present in the sample so that it can be processed to obtain good-quality UV spectra.

On the other hand, the shifts in λ_{max} values were not consistent across different conjugations. The methylation at a particular hydroxyl position in the structure of flavones or flavonols did not cause similar shifts in λ_{max} as the substitution by glucuronic acid at the same position (see Figure S2, SI). Sulfates of 4′HF, 5HF, and 7HF did not always lead to similar shifts in λ_{max} as glucuronides (data not shown here). Therefore, a systematic study on monosulfates of flavonoids is required to define the diagnostic shifts in λ_{max} on the basis of position of sulfation.

In conclusion, we developed a λ_{max} shift method to identify the position of glucuronidation for mono-*O*-glucuronides of flavones and flavonols, and this method is simpler and faster than NMR or EI-MS/CID coupled with metal complexation. This method does not require the purification of glucuronides or the use of shift regents. The only requirements are sufficient amounts (~1−5 μM) of metabolites and aglycones to generate good-quality spectra and that the position of the hydroxyl group is at 3, 4′, 5, and/or 7, single or in combination. Information about the position of glucuronidation is expected to serve as a very important tool in furthering the study of metabolism by UGT isoforms and the role of efflux transporters in the excretion of glucuronides.

ABBREVIATIONS USED

UGT, UDP-glucuronosyltransferase; UDPGA, uridine diphosphoglucuronic acid; UPLC, ultraperformance liquid chromatography; MS, mass spectroscopy; NMR, nuclear magnetic resonance; UV, ultraviolet; PDA, photodiode array detector; SMR, structure−metabolism relationship; HF, hydroxyflavone; DHF, dihydroxyflavone; THF, trihydroxyflavone; MHF, methoxyhydroxyflavone; DMHF, dimethoxyhydroxyflavone; DHMF, dihydroxymethoxyflavone; MRP2, multiresistance protein 2; BCRP, breast cancer resistance protein; SI, Supporting Information; EI-MS/CID, electrospray ionization mass spectrometry coupled with collision-induced dissociation.

Supporting Information Available: UPLC chromatograms and LC/MS/MS scans of 3HF, 3,5DHF, 3,7DHF, 3,5,7THF 3,7,4′THF (resokaempferol), and 3,5,7,4′-tetrahydroxyflavone (kaempferol) (and their glucuronides; UV spectra of 36 selected flavonoids and their corresponding glucuronides; and UPLC/MS/MS optimized ion source and compound parameters for precursor ion scan for 3HF, 3,4′DHF, 3,5DHF, 3,7DHF, 3,5,7THF 3,7,4′THF (resokaempferol) and 3,5,7,4′-tetrahydroxyflavone (kaempferol). This material is available free of charge via the Internet at http://pubs.acs.org.

LITERATURE CITED

(1) Kelly, G. E.; Joannou, G. E.; Reeder, A. Y.; Nelson, C.; Waring, M. A. The variable metabolic response to dietary isoflavones in humans. *Proc. Soc. Exp. Biol. Med.* **1995**, *208* (1), 40–43.

(2) Busby, M. G.; Jeffcoat, A. R.; Bloedon, L. T.; Koch, M. A.; Black, T.; Dix, K. J.; Heizer, W. D.; Thomas, B. F.; Hill, J. M.; Crowell, J. A.; Zeisel, S. H. Clinical characteristics and pharmacokinetics of purified soy isoflavones: single-dose administration to healthy men. *Am. J. Clin. Nutr.* **2002**, *75* (1), 126–136.

(3) Walle, T. Absorption and metabolism of flavonoids. *Free Radical Biol. Med.* **2004**, *36* (7), 829–837.

(4) Feng, W. Y. Metabolism of green tea catechins: an overview. *Curr. Drug Metab.* **2006**, *7* (7), 755–809.

(5) Erlund, I.; Kosonen, T.; Alfthan, G.; Maenpaa, J.; Perttunen, K.; Kenraali, J.; Parantainen, J.; Aro, A. Pharmacokinetics of quercetin from quercetin aglycone and rutin in healthy volunteers. *Eur. J. Clin. Pharmacol.* **2000**, *56* (8), 545–553.

(6) Sesink, A. L.; O'Leary, K. A.; Hollman, P. C. Quercetin glucuronides but not glucosides are present in human plasma after consumption of quercetin-3-glucoside or quercetin-4′-glucoside. *J. Nutr.* **2001**, *131* (7), 1938–1941.

(7) Williamson, G.; Manach, C. Bioavailability and bioefficacy of polyphenols in humans. II. Review of 93 intervention studies. *Am. J. Clin. Nutr.* **2005**, *81* (1 Suppl.), 243S–255S.

(8) Manach, C.; Williamson, G.; Morand, C.; Scalbert, A.; Remesy, C. Bioavailability and bioefficacy of polyphenols in humans. I. Review of 97 bioavailability studies. *Am. J. Clin. Nutr.* **2005**, *81* (1 Suppl.), 230S–242S.

(9) Nettleton, J. A.; Greany, K. A.; Thomas, W.; Wangen, K. E.; Adlercreutz, H.; Kurzer, M. S. Plasma phytoestrogens are not altered by probiotic consumption in postmenopausal women with and without a history of breast cancer. *J. Nutr.* **2004**, *134* (8), 1998–2003.

(10) Hu, M.; Chen, J.; Lin, H. Metabolism of flavonoids via enteric recycling: mechanistic studies of disposition of apigenin in the Caco-2 cell culture model. *J. Pharmacol. Exp. Ther.* **2003**, *307* (1), 314–321.

(11) Chen, J.; Lin, H.; Hu, M. Metabolism of flavonoids via enteric recycling: role of intestinal disposition. *J. Pharmacol. Exp. Ther.* **2003**, *304* (3), 1228–1235.

(12) Walle, T.; Otake, Y.; Brubaker, J. A.; Walle, U. K.; Halushka, P. V. Disposition and metabolism of the flavonoid chrysin in normal volunteers. *Br. J. Clin. Pharmacol.* **2001**, *51* (2), 143–146.

(13) Perabo, F. G.; Von Low, E. C.; Ellinger, J.; von Rucker, A.; Muller, S. C.; Bastian, P. J. Soy isoflavone genistein in prevention and

treatment of prostate cancer. *Prostate Cancer Prostatic Dis*. **2008**, *11* (1), 6–12.
(14) Liu, Y.; Hu, M. Absorption and metabolism of flavonoids in the Caco-2 cell culture model and a perused rat intestinal model. *Drug Metab. Dispos*. **2002**, *30* (4), 370–377.
(15) Hollman, P. C.; Katan, M. B. Absorption, metabolism and health effects of dietary flavonoids in man. *Biomed. Pharmacother*. **1997**, *51* (8), 305–310.
(16) Miners, J. O.; Smith, P. A.; Sorich, M. J.; McKinnon, R. A.; Mackenzie, P. I. Predicting human drug glucuronidation parameters: application of in vitro and in silico modeling approaches. *Annu. Rev. Pharmacol. Toxicol*. **2004**, *44*, 1–25.
(17) Burchell, B. Transformation reactions: glucuronidation. In *Handbook of Drug Metabolism*; Woolf, T. F., Ed.; Dekker: New York, 1999; pp xi, 596 p.
(18) Joseph, T. B.; Wang, S. W.; Liu, X.; Kulkarni, K. H.; Wang, J.; Xu, H.; Hu, M. Disposition of flavonoids via enteric recycling: enzyme stability affects characterization of prunetin glucuronidation across species, organs, and UGT isoforms. *Mol. Pharmaceutics* **2007**, *4* (6), 883–894.
(19) Davis, B. D.; Needs, P. W.; Kroon, P. A.; Brodbelt, J. S. Identification of isomeric flavonoid glucuronides in urine and plasma by metal complexation and LC-ESI-MS/MS. *J. Mass Spectrom*. **2006**, *41* (7), 911–920.
(20) Davis, B. D.; Brodbelt, J. S. Regioselectivity of human UDP-glucuronosyl-transferase 1A1 in the synthesis of flavonoid glucuronides determined by metal complexation and tandem mass spectrometry. *J. Am. Soc. Mass Spectrom*. **2008**, *19* (2), 246–256.
(21) Cuyckens, F.; Claeys, M. Determination of the glycosylation site in flavonoid mono-*O*-glycosides by collision-induced dissociation of electrospray-generated deprotonated and sodiated molecules. *J. Mass Spectrom*. **2005**, *40* (3), 364–372.
(22) Dueñas, M.; Mingo-Chornet, H.; Pérez-Alonso, J. J.; Paola-Naranjo, R. D.; González-Paramás, A. M.; Santos-Buelga, C. Preparation of quercetin glucuronides and characterization by HPLC−DAD−ESI/MS. *Eur. Food Res. Technol*. **2008**, *227* (4), 1069–1076.
(23) Wittig, J.; Herderich, M.; Graefe, E. U.; Veit, M. Identification of quercetin glucuronides in human plasma by high-performance liquid chromatography−tandem mass spectrometry. *J. Chromatogr., B: Biomed. Sci. Appl*. **2001**, *753* (2), 237–243.
(24) Mullen, W.; Boitier, A.; Stewart, A. J.; Crozier, A. Flavonoid metabolites in human plasma and urine after the consumption of red onions: analysis by liquid chromatography with photodiode array and full scan tandem mass spectrometric detection. *J. Chromatogr., A* **2004**, *1058* (1−2), 163–168.
(25) Day, A. J.; Bao, Y.; Morgan, M. R.; Williamson, G. Conjugation position of quercetin glucuronides and effect on biological activity. *Free Radical Biol. Med*. **2000**, *29* (12), 1234–1243.
(26) Mabry, T. J.; Markham, K. R.; Thomas, M. B. *The Systematic Identification of Flavonoids*; Springer-Verlag: New York, 1970; pp xi, 354.
(27) Tang, L.; Singh, R.; Liu, Z.; Hu, M. Structure and concentration changes affect characterization of UGT isoform-specific metabolism of isoflavones. *Mol. Pharmaceutics* **2009**, *6* (5), 1466–1482.
(28) Liu, X.; Tam, V. H.; Hu, M. Disposition of flavonoids via enteric recycling: determination of the UDP-glucuronosyltransferase isoforms responsible for the metabolism of flavonoids in intact Caco-2 TC7 cells using siRNA. *Mol. Pharmaceutics* **2007**, *4* (6), 873–882.
(29) King, R.; Fernandez-Metzler, C. The use of Qtrap technology in drug metabolism. *Curr. Drug Metab*. **2006**, *7* (5), 541–545.
(30) Clarke, N. J.; Rindgen, D.; Korfmacher, W. A.; Cox, K. A. Systematic LC/MS metabolite identification in drug discovery. *Anal. Chem*. **2001**, *73* (15), 430A–439A.
(31) Markham, K. R. *Techniques of Flavonoid Identification*; Academic Press: London, U.K., 1982; pp xi, 113.
(32) Boersma, M. G.; van der Woude, H.; Bogaards, J.; Boeren, S.; Vervoort, J.; Cnubben, N. H.; van Iersel, M. L.; van Bladeren, P. J.; Rietjens, I. M. Regioselectivity of phase II metabolism of luteolin and quercetin by UDP-glucuronosyl transferases. *Chem. Res. Toxicol*. **2002**, *15* (5), 662–670.
(33) Day, A. J.; Mellon, F.; Barron, D.; Sarrazin, G.; Morgan, M. R.; Williamson, G. Human metabolism of dietary flavonoids: identification of plasma metabolites of quercetin. *Free Radical Res*. **2001**, *35* (6), 941–952.
(34) van der Woude, H.; Boersma, M. G.; Vervoort, J.; Rietjens, I. M. Identification of 14 quercetin phase II mono- and mixed conjugates and their formation by rat and human phase II in vitro model systems. *Chem. Res. Toxicol*. **2004**, *17* (11), 1520–1530.
(35) Jeong, E. J.; Lin, H.; Hu, M. Disposition mechanisms of raloxifene in the human intestinal Caco-2 model. *J. Pharmacol. Exp. Ther*. **2004**, *310* (1), 376–385.
(36) Smith, P. A.; Sorich, M. J.; McKinnon, R. A.; Miners, J. O. Pharmacophore and quantitative structure−activity relationship modeling: complementary approaches for the rationalization and prediction of UDP-glucuronosyltransferase 1A4 substrate selectivity. *J. Med. Chem*. **2003**, *46* (9), 1617–1626.
(37) Williamson, G.; Aeberli, I.; Miguet, L.; Zhang, Z.; Sanchez, M. B.; Crespy, V.; Barron, D.; Needs, P.; Kroon, P. A.; Glavinas, H.; Krajcsi, P.; Grigorov, M. Interaction of positional isomers of quercetin glucuronides with the transporter ABCC2 (cMOAT, MRP2). *Drug Metab. Dispos*. **2007**, *35* (8), 1262–1268.

Received for review December 29, 2009. Revised manuscript received May 24, 2010. Accepted July 12, 2010. This work was supported by NIH Grant GM070737 and a training fellowship from the Pharmacoinformatics Training Program of the Keck Center of the Gulf Coast Consortia (NIH Grant 5 R90 DK071505-03).